Vol. 04, Iss. 2 (2026) 155-168, DOI: 10.61552/JME.2026.02.003

JME

Journal of Materials and Engineering

www.jme.aspur.rs

Research article

Performance Analysis of AISI 1040 Steel Turning Under Al_2O_3–ZnO Hybrid Nanofluid MQL Using Response Surface Methodology - A Step Towards Sustainable Machining

Altaf Nalbandh[a,b], Neeraj Chavda[a,c,*], Rakesh Bumataria[b]

[a]*Gujarat Technological University (GTU), Ahmedabad, Gujarat, India,*

[b]*Mechanical Engineering Department, Government Polytechnic, Porbandar, Gujarat, India,*

[c]*Mechanical Engineering Department, G. H. Patel College of Engineering and Technology, The Charutar Vidya Mandal (CVM) University, Vallabh Vidhyanagar, Anand, Gujarat, India.*

Keywords:

Hybrid nanofluids
MQL
Response surface methodology
ANOVA
Al_2O_3
ZnO

* Corresponding author:

Neeraj Chavda
E-mail: neeraj_chavda@yahoo.com

Received: 12 January 2026
Revised: 18 February 2026
Accepted: 19 March 2026

A B S T R A C T

UN's SDG 9 aims to promote cleaner production and more resource efficient industrial processes. Environment-friendly cutting fluids play a crucial role in cutting operations by addressing environmental and health concerns for users. Nanofluid is a sustainable product that also encourages near-dry machining using minimum quantity lubrication (MQL). This study investigates the effect of an Al_2O_3–ZnO hybrid nanofluid applied through MQL on the turning performance of AISI 1040 steel. Cutting Speed, feed rate, and nanoparticle weight percentage were selected as control factors, while cutting force, cutting temperature, and surface roughness were considered as output responses. The experiments were planned using Response Surface Methodology (RSM) based on a Box–Behnken design for different cooling conditions and varying proportional ratios of Al_2O_3–ZnO nanoparticles to capture main and interaction effects among the process parameters. Analysis of variance confirmed the statistical significance and adequacy of the proposed models for all responses. The hybrid nanofluid cooling condition (75:25, Al_2O_3–ZnO) under MQL led to notable reductions in cutting temperature and surface roughness, along with lower cutting forces compared with conventional cutting conditions reported in this research. The multi-response optimization indicated that low cutting speed (31.71 m/min), low feed rate (0.18 mm/rev), and an intermediate nanoparticle weight percentage (1 wt%) provide the best compromise among cutting force, temperature, and surface roughness. The results highlight the potential of Al_2O_3–ZnO hybrid nanofluid-based MQL as a promising and sustainable cutting environment for improving machinability and surface integrity in steel turning operations. This encourages the use of such sustainable techniques in metal machining.

1. INTRODUCTION

The turning of medium carbon steels such as AISI 1040 is widely employed in automotive and general engineering components that demand reliable dimensional accuracy, low surface roughness, and controlled cutting forces. Conventional flood cooling systems enhance heat dissipation and lubrication. However, they are increasingly criticized for their high consumption, disposal issues, and adverse environmental and health impacts, which have motivated the adoption of more sustainable lubrication and cooling strategies. In addition, the accessibility of cutting fluid within the cutting zone is a concern. The flood-cooling constraints could be circumvented by replacing the cutting fluid with wet machining, as in dry machining [1]. A novel, economical, and practical approach to MQL machining technology has been developed to eliminate the issues above, which are produced by conventional cutting fluids in the metal industry [2]. The alternative strategy of mist lubrication, where an air-cutting fluid mixture is supplied to the cutting zone and is more readily accessible due to the high pressure, has proven to be a superior option for coolant system applications [3]. The nozzle was used to mix the lubricant/coolant with oil, producing an aerosol. To achieve better cooling, spray the aerosol into the cutting zone at high pressure [4]. MQL has emerged as an attractive alternative that delivers a small amount of lubricant directly to the cutting zone, thereby reducing fluid usage while maintaining adequate lubrication.

Nanofluids, formed by dispersing solid nanoparticles in a base fluid, can significantly enhance the thermal and tribological performance of MQL systems by improving heat transfer and reducing friction at the tool–chip interface. Hybrid nanofluids, such as Al_2O_3–ZnO suspensions, combine different nanoparticles to exploit synergistic effects, offering higher thermal conductivity, better stability, and improved anti-wear and anti-friction behavior compared with mono-nanofluids [5, 6]. These characteristics can translate into lower cutting temperatures, reduced cutting forces, and improved surface quality in metal cutting processes. However, the combined influence of process parameters and nanoparticle concentration on multi-response machinability in turning AISI 1040 under MQL remains insufficiently quantified.

Response Surface Methodology (RSM), particularly the Box–Behnken design, provides an efficient framework for modeling and optimizing complex machining processes with a limited number of experiments by developing empirical relationships between inputs and multiple responses.

Sharma et al. [7] performed experimentation for analyzing the impact of Al_2O_3 (45 nm) and MoS_2 (30 nm) with a fraction of 9:1 to get a dispersed hybrid nanofluid in the turning operation of AISI 304 steel. Nanoparticle fractions of 0.25, 0.75, and 1.25 v% were employed. Significant retardation in Fx. Fy, Fz, and Ra were 18.08%, 5.73%, 7.35%, and 2.38%, respectively. Singh et al. [8] conducted simulations of the impact of incorporating graphene nanoplatelets into an Al-based nanofluid at concentrations of 0.25, 0.75, and 1.25 v% to construct a hybrid nanofluid. With an enhancement in nanoparticle concentration, thermal conductivity, viscosity, and wear were all improved. The results of comparing an alumina-based nanofluid with the base fluid demonstrate that the hybrid has superior wettability. The results showed a 20.28% decrease in surface roughness, a 17.38% reduction in thrust force, a 9.94% decrease in cutting force, and a 7.25% decrease in feed force. Sharma et al. [9] checked the impact of hybrid nanofluids made of Al_2O_3 and GnP in turning AISI 304 steel. Hybrid nanofluids were developed at concentrations of 0.25, 0.75, and 1.25 v%. Hybrid nanofluids had the lowest pin wear and friction coefficient, as determined by tribological and wettability testing. Results revealed a retardation of 5.29% in cutting temperature and 12.29% in tool wear with nanofluids compared to Al-based nanofluid. Jamil et al. [10], studied the usefulness of cryogenic cooling (CO2) and minimum quantity lubrication in turning tungsten alloys. Al_2O_3 (30 nm) and MWCNT (10-30 nm) are suspended in a vegetable oil-based fluid for nanofluid preparation. Taguchi's L9 orthogonal array was used for experiments design using with cutting Speed, feed rate, and cooling techniques as design variables. It was seen from the results that the mean surface roughness was retard by 8.72%, the machining cutting force by 11.8%, and the tool life was enhanced by 23% with hybrid nanofluids in contrast to CO2 cooling. Although a retardation of 11.2% in cutting temperature was seen with CO_2 cooling compared to hybrid nanofluid-based MQL. Yildirim [11] experimentally investigated the effects of cooling conditions, notably dry, minimum quantity lubrication, cryogenic, nanofluids, and combinations of these approaches on the turning of Inconel 625. Al_2O_3 (70 nm) and hBN (70 nm) were incorporated into the nanofluid in various concentration ratios. LN2 worked better for cryogenic cooling. Surface roughness, tool wear, and tool-chip junction temperature were the output parameters. The results indicate that employing the 0.5 v% hBN cooling approach in addition to LN2 was the optimum combination for enhanced manufacturing. Thakur et al. [12] studied the results of turning EN 24 steel using various cooling methods, including minimum quantity lubrication, MQLNF, and minimum quantity lubrication. Al_2O_3, CuO, and Al-CuO nanoparticles were added to water at a fraction of 0.2, 0.4, and 0.6wt%, respectively, to create nano-fluids and hybrid nano-fluids. The thermal conductivity of hybrid nanofluids was discovered to be greater than that of either mono nanofluid. The experiments showed that using a hybrid nanofluid + minimum quantity lubrication reduced the coefficient of friction, surface roughness, cutting temperature, and tool wear. Thakur et al. [13] experimentally evaluated the impact of turning EN 24 steel from different cooling methods, MQL, nanofluids + MQL, and composite nanofluids + MQL. Water was enriched with 0.5, 1, and 1.5 percent of Al_2O_3, CuO, and Al-CuO nanoparticles, respectively. After a comparison investigation, the hybrid nanofluids performed better than the nanofluids. Gugulothuet al. [14] experimentally studied sedimentation tests and characterization of nanofluids, which were prepared using CNT (30 nm) and MoS2 (30 nm) nanoparticles in 0.5, 1, 1.5, 2, 2.5, and 3wt% concentration in sesame oil as a base fluid. These NFs were used in machining under MQL to turn AISI 1040 steel with an uncoated carbide tool. Results revealed retardation in the coefficient of friction, thrust force, feed force, main cutting force, and surface roughness at 2 wt% of CNT+MoS_2 hybrid cutting nano-fluids compared to dry and conventional cutting fluids. Furthermore, cutting temperature and tool wear was retard at 3wt% of CNT+MoS_2 hybrid cutting nano-fluids in contrast with dry machining and conventional cutting fluid machining. Zaman et al. [15] studied the influence of cutting Speed, feed rate, depth of cut, nanoparticle concentration, and tool type on cutting temperatures and surface roughness in the turning of Ti-6Al-4V alloy under hybrid Al_2O_3-MWCNT nanofluid-based MQL. The Box-Behnken method was implemented in the experiment design. Empirical models were established employing RSM. The temperature improved with cutting Speed, depth of cut, and feed rate, consistent with estimations and experimental results. However, while the particle proportions increased, the temperature dropped to its lowest possible level and then rose further. The most crucial factor regarding roughness was the machine feed rate. Sandeep Kumar et al. [16] studied the impact of hybrid nanofluids with Cu-Zn with base fluid as a groundnut oil with an application of MQL in turning operation of Inconel 718 with a cutting tool fitted with a Ti-coated insert. In experimentation, input machining parameters were applied under conditions such as dry, MQL with vegetable oil, and MQL with nanofluid. From the investigation, it is found that retardation in cutting temperature and surface roughness in MQL + nanofluid, compared with dry and MQL + vegetable oil cooling conditions. Sandeep Kumar et al. [17] conducted tests using CuO + ZnO (50:50) hybrid nanoparticles in vegetable oils, such as palm oil and coconut oil, as the base fluid for machining AISI 1018 steel. In experimentation, the performance of hybrid nano cutting fluids was compared with the dry machining process, and notable retardation in surface roughness; feed was the main indicating parameter compared to the cut and cutting speed depth. Haghnazari & Abedini [18] processed parameters in machining of AISI 4340 steel with input parameters as rotational Speed, feed rate, and hybrid nanofluid with different weight percentages from 0 to 1 of CuO (in a mixture of Al_2O_3 and CuO) using MQL and investigated the effect on output parameters such as machining force and surface roughness. The composition of (75:25, Al_2O_3:CuO) showed the lowest value of machining force at lower feed and higher rpm, and the lowest value of surface roughness at lower feed and moderate rpm.

In this work, cutting speed, feed rate, and nanoparticle weight percentage in an Al_2O_3–ZnO hybrid nanofluid-based MQL system are considered as input factors, while cutting force, cutting temperature, and surface roughness constitute the output responses. The objective is to develop statistically significant models, analyze the influence of main and interaction effects, and determine optimal cutting conditions that enhance machining performance and support sustainable manufacturing. The effect of varying nanoparticle concentration has been studied.

2. MATERIALS AND METHODS

In this study, a design of experiments (DOE) using the response surface method (RSM) is conducted to investigate the effects of output parameters.

DOE facilitates the study of operations and reduces costs and time. In DOE, three input control factors are cutting speed, fees, and wt% concentration of different hybrid nanofluids. The factor cutting speed has three levels of 31.71, 69.63, and 107.55, factor feed has three levels of 0.11, 0.18, and 0.25, and factor wt% has three levels of 0, 1, and 2. All input parameters and their levels are given in Table 1. The base fluid used for this study is SAE-40, a single-grade oil.

Table 1. RSM Box Behnken Method input parameters with their level.

Input parameters	Low (-1)	High (1)	Center (0)
Cutting Speed (m/min)	31.71	107.55	69.63
Feed (mm/rev)	0.11	0.25	0.18
Wt% of nanoparticle (%)	0	2	1

In this experiment, the two-step method of nanofluid preparation is used, with prepared NPs mixed with 100 ml of SAE-40 oil as the base fluid. There are two types of nanoparticles (NPs) used for hybrid nanofluid (HyNF) preparation: Aluminium Oxide (Al_2O_3) and Zinc Oxide (ZnO). The technical specifications for both NP are given in Table 2. For HyNF preparation and NPs stability in base fluid, magnetic stirrers and an ultrasonic homogenizer were used. This mixture was placed in a magnetic stirrer; it stirred for 2 hours. After this step, the mixture was sonicated in an ultrasonic homogenizer for 2 hours.

Table 2. Nanoparticle technical specification.

Technical Specifications	Aluminium Oxide	Zinc Oxide
Molecular Formula	Al_2O_3	ZnO
Purity (%)	99.90	99.90
Average particle size (nm)	30-50	30-50
True Density (g/cm^3)	3.97	4.97
Bulk Density (g/cm^3)	1.5	-
Specific Surface area (m2/g)	120-140	90-110
Molecular Weight (g/mol)	101.96	81.408
Morphology	Spherical	Spherical
Colour	White	Milky White
Physical form	Powder	Powder

To spray NF as a cutting fluid in the cutting zone, the MQL system has been utilized. The typical MQL includes a bowl reservoir, a pressure control valve, a mixing chamber to control the flow of NF, and a 2 mm nozzle. In this study, air pressure is kept constant at 3 bar, and the flow rate is 360 ml/hr. A workpiece measuring Ø50 × 300 mm of AISI 1040 steel is used in the experiments. Table 3 provides workpiece composition.

Table 3. Chemical composition (%) of workpiece.

C	Si	Mn	P	S	Cr	Mo	Ni
0.4-0.45	0.05-0.35	0.7-0.9	0.027	0.017	0.232	0.08	0.048

Table 4. Details of experimentation and cutting conditions.

Workpiece	
Material	AISI 1040 steel
Size	50 mm (Diameter) × 300 mm (Length)
Cutting fluid	
Cutting fluid	SAE-40 oil
Nanoparticle	
Aluminum Oxide (Al_2O_3)	30-50 nm
Zinc Oxide (ZnO)	30-50 nm
Weight percentage of nanoparticles	0%, 1%, 2%
Input machining parameters	
Cutting Speed	31.71, 69.63, 107.55 m/min
Feed rate	0.11, 0.18, 0.25 mm/rev
Depth of cut	0.6 mm
MQL	
Nozzle diameter	2 mm
Nano fluid discharge	360 ml/hr
Air Pressure	3 bar
Machine tools and measuring devices	
Lathe	Banka 35 750 geared type
Cutting tool (insert)	Deskar TNMG160408 CQ LF9218
Cutting force	Dynamometer strain gauge-based bridged form type
Cutting temperature	Fluke 62 Max+ digital infrared thermometer
Surface Roughness	Mitutoyo SJ-210 portable tester

In this research, Banka 35 750 geared lathe machine of Banka Machine Pvt. Ltd. is used for turning, and the tool used is Deskar TNMG160408 CQ LF9218. The strain gauge-based bridged form type lathe tool dynamometer to measure cutting force. Also, a Fluke 62 Max+ digital infrared thermometer is used to measure cutting temperature, and a portable surface roughness tester SJ-210 of Mitutoyo is used to measure the surface roughness of the workpiece. In all runs of experiments, the depth of cut is kept fixed at 0.6 mm. Table 4 provides detailed specifications of experiments. Fig. 1 shows the detailed experimental setup.

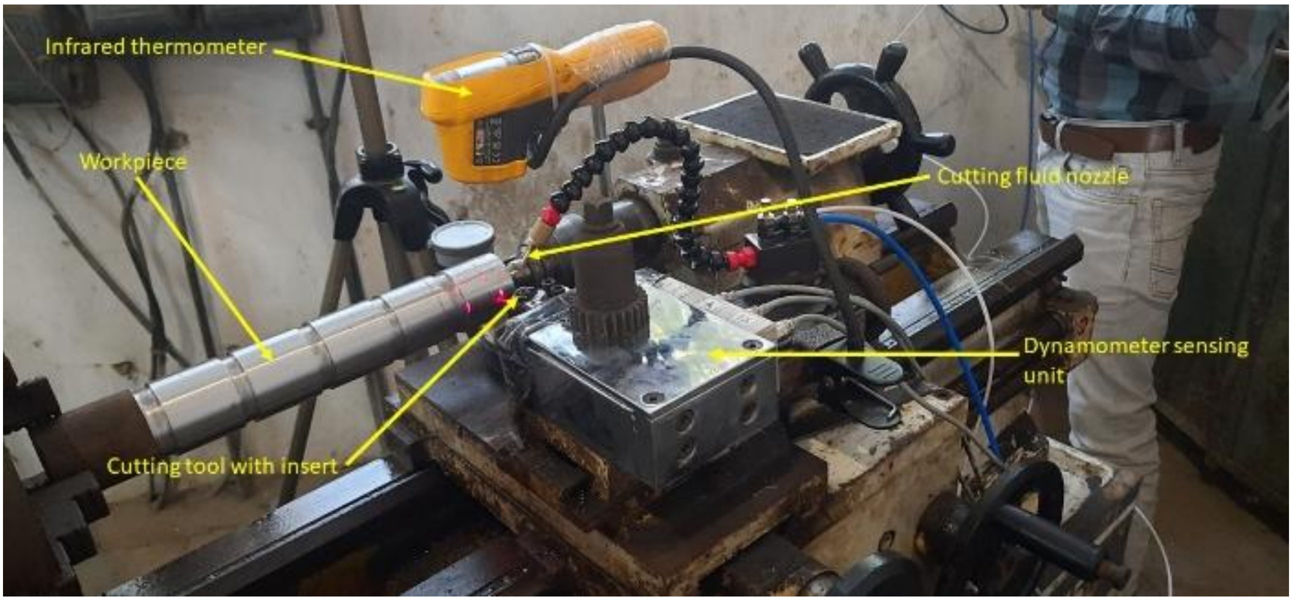

Fig. 1. Experimental setup.

Box Behnken method is used for applying RSM in experimentation. 17 experiments have been designed for each type of cooling method. Different cooling methods with proportional mixing ratios of two NPs are given in Table 5.

Table 5. Cooling methods with proportional ratio mixing of nanoparticles.

Cooling method	Proportional ratio of nanoparticles
Case A	Al_2O_3:ZnO (25:75)
Case B	Al_2O_3:ZnO (50:50)
Case C	Al_2O_3:ZnO (75:25)

3. RESULT AND DISCUSSION

Three different cooling methods (Case A, Case B, and Case C), three input parameters such as cutting speeds (31.71, 69.93, and 107.55 m/min), feeds (0.11, 0.18, and 0.25 mm/rev), and weight percent (0,1, and 2 wt%) were used in total 51 experiments conducted on AISI 1040 steel. Cutting force, cutting temperature, and surface roughness are measured for each test run and cooling method. RSM test runs, input and output values for Case A, Case B, and Case C are given in Table 6, Table 7, and Table 8, respectively.

Table 6. RSM test run, input and output values for Case A.

Test Run	Input parameters			Output parameters		
	A:Cutting Speed	B:Wt% of NP	C:Feed	Cutting Force	Cutting Temperature	Surface Roughness
	m/min	%	mm/rev	N	°C	µm
1	107.55	0	0.18	303.99	97.84	3.599
2	31.71	0	0.18	320.36	66.17	3.563
3	69.63	1	0.18	214.06	68.33	3.864
4	31.71	2	0.18	207.59	50.5	4.49
5	31.71	1	0.25	253.29	59	4.64
6	69.63	1	0.18	223.58	68.53	3.892
7	69.63	1	0.18	218.38	69.33	3.86
8	69.63	1	0.18	251.13	76.26	4.246

9	69.63	2	0.11	135.72	49.08	3.584
10	31.71	1	0.11	147.09	51	2.67
11	69.63	0	0.25	392.24	93.33	4.54
12	69.63	2	0.25	282.71	46	5.026
13	69.63	1	0.18	239.76	75.16	4.182
14	69.63	0	0.11	317.81	80.82	3.318
15	107.55	1	0.11	147.09	69.67	2.621
16	107.55	1	0.25	243.48	75.67	4.688
17	107.55	2	0.18	241.82	58.83	4.312

Table 7. RSM test run, input and output values for Case B.

Test Run	Input parameters			Output parameters		
	A:Cutting Speed	B:Wt% of NP	C:Feed	Cutting Force	Cutting Temperature	Surface Roughness
	m/min	%	mm/rev	N	°C	μm
1	107.55	0	0.18	303.99	97.84	3.599
2	31.71	0	0.18	338.31	72	4.269
3	69.63	1	0.18	237.01	58	4.242
4	31.71	2	0.18	231.23	53.61	4.297
5	31.71	1	0.25	287.61	50.17	4.559
6	69.63	1	0.18	245.15	60.33	3.958
7	69.63	1	0.18	235.34	60.27	4.16
8	69.63	1	0.18	260.74	65	4.339
9	69.63	2	0.11	145.42	49.08	3.78
10	31.71	1	0.11	166.70	46.83	3.974
11	69.63	0	0.25	392.24	93.33	4.54
12	69.63	2	0.25	265.94	62.22	4.68
13	69.63	1	0.18	250.05	59.8	4.142
14	69.63	0	0.11	295.16	80.82	3.489
15	107.55	1	0.11	166.70	58.87	3.539
16	107.55	1	0.25	253.29	63.33	4.07
17	107.55	2	0.18	233.28	70.88	4.068

Table 8. RSM test run, input and output values for Case C.

Test Run	Input parameters			Output parameters		
	A:Cutting Speed	B:Wt% of NP	C:Feed	Cutting Force	Cutting Temperature	Surface Roughness
	m/min	%	mm/rev	N	°C	μm
1	107.55	0	0.18	303.99	97.84	3.719
2	31.71	0	0.18	337.23	69.55	3.69
3	69.63	1	0.18	233.68	55.27	4.159
4	31.71	2	0.18	294.18	55.55	4.143
5	31.71	1	0.25	346.45	53.03	4.712
6	69.63	1	0.18	243.48	56.54	4.159
7	69.63	1	0.18	250.05	56.73	4.223
8	69.63	1	0.18	257.02	60.8	4.375
9	69.63	2	0.11	150.33	54.06	3.701
10	31.71	1	0.11	148.76	43.21	2.996
11	69.63	0	0.25	392.24	93.33	4.54
12	69.63	2	0.25	346.84	62.72	4.979
13	69.63	1	0.18	245.15	58	4.267
14	69.63	0	0.11	297.81	80.82	3.318
15	107.55	1	0.11	156.90	56.47	3.867
16	107.55	1	0.25	269.67	64.49	4.546
17	107.55	2	0.18	259.27	63.75	4.845

Analysis of Variance (ANOVA) results are obtained from software for output response of cutting force, cutting temperature, and surface roughness for each cooling condition, i.e., Case A, Case B, and Case C. Model for each parameter for each case was found significant, and the residual was not significant. The values of R-Sq (R^2) and Adj R-Sq (Adjusted R^2) derived from ANOVA Fit Statistics are shown in Fig. 2.

As shown in Fig. 2, Case C has a high value of R-Sq and Adj R-Sq as compared to Case A and Case B for all output responses: Cutting Force (0.9781 and 0.9499), Cutting Temperature (0.9859 and 0.9677), and Surface Roughness (0.9549 and 0.9278). It is desirable that R-Sq and Adj R-Sq should be as high as possible. Case C will be the most suitable case considered for further analysis.

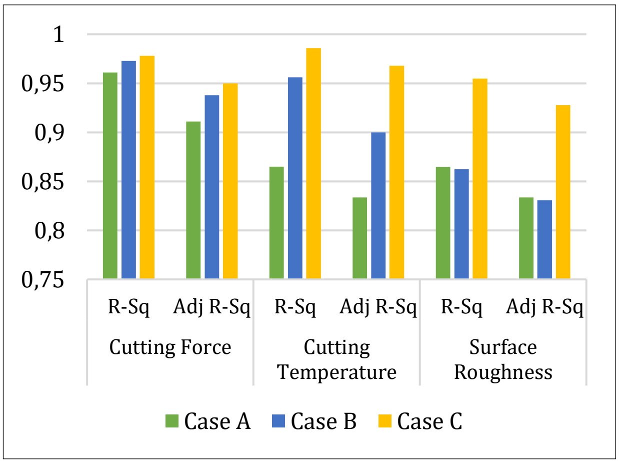

Fig. 2. ANOVA Fit Statistics for all cooling conditions.

3.1 Analysis of output parameters for Case C

In this experimental study, cutting force and cutting temperature were analyzed during the turning operation, whereas surface roughness was analyzed after the end of the operation. Additionally, statistical analysis was carried out using Design-Expert 13 software (at a 95% desirability level) for output responses and for plotting normal probability, residuals vs run, pretribulation, and 3D surface plots. Finally, a discussion of statistical analysis of the effects on output parameters by influencing them. For Case C i.e., Al_2O_3:ZnO (75:25), analysis of variance (ANOVA) results obtained from regression analysis for response of cutting force, cutting temperature, and surface roughness, and models predicted by software are discussed in the following sections.

3.1.1 Cutting Force

The software predicts a quadratic model, and it is meaningful, as the p-value is less than 0.05. It means that the lower the p-value of a factor, the more meaningful it is relative to the other factors. From Table 9, the ANOVA for cutting force indicates that the feed is more significant (p-value < 0.0001) than wt% of NP (p-value = 0.0004) and cutting speed (p-value = 0.0178). Also, in this quadratic model, the square of wt% of NP has a p-value equal to 0.0001, which has a greater effect, followed by wt% of NP. This model is a suitable model for output response cutting force drawn out from the data in Table 9. The Eq.1 shows final model for cutting force output response.

Table 9. ANOVA for cutting force.

Source	Sum of Squares	Mean Square	F-value	p-value	
Model	76942.88	8549.21	34.68	< 0.0001	significant
A-Cutting Speed	2339.06	2339.06	9.49	0.0178	
B-Wt% of NP	9845.39	9845.39	39.94	0.0004	
C-Feed	45210.54	45210.54	183.41	< 0.0001	
AB	0.6947	0.6947	0.0028	0.9591	
AC	1802.85	1802.85	7.31	0.0304	
BC	2605.11	2605.11	10.57	0.0140	
A^2	193.88	193.88	0.7865	0.4046	
B^2	14944.60	14944.60	60.63	0.0001	
C^2	314.96	314.96	1.28	0.2956	
Residual	1725.51	246.50			
Lack of Fit	1428.91	476.30	6.42	0.0521	not significant
Pure Error	296.60	74.15			
Cor Total	78668.40				

$$\begin{aligned} Cutting\ Force = 245.88 &- 17.10 \times Cutting\ Speed - 35.08 \times wt\%\ of\ NP + 75.18 \times Feed \\ &- 0.4168 \times Cutting\ Speed \times wt\%\ of\ NP - 21.23 \times Cutting\ Speed \times Feed \\ &+ 25.52 \times wt\%\ of\ NP \times Feed - 6.79\ (Cutting\ Speed)^2 + 59.58 \times (wt\%\ of\ NP)^2 \\ &- 8.65\ (Feed)^2 \end{aligned} \tag{1}$$

The normal probability plot for cutting force is shown in Fig. 3 and indicates that residuals have a close distance from the straight line. The terminology mentioned in the model is significant [19]. The externally studentized residuals versus run plot in Fig. 4 indicates a range of -4.8193 to 4.8193. It means this fitted model is suitable for cutting force response.

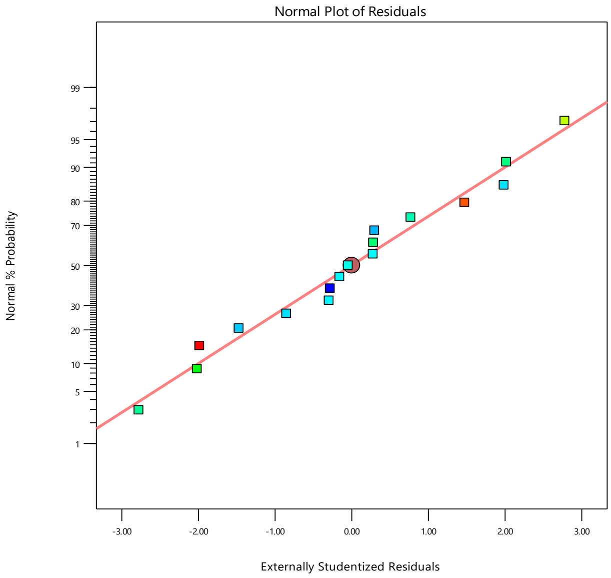

Fig. 3. Normal % probability plot for cutting force.

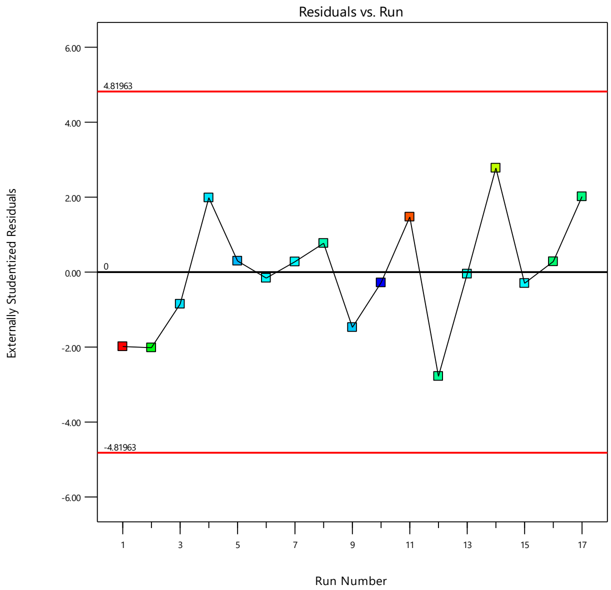

Fig. 4. Externally studentized residuals vs run of experiments.

Fig. 5 shows the effect of all input parameters: A: cutting Speed of 69.63 m/min, B: 1 wt% of NP, and C: feed of 0.18 mm/rev. As the feed rate increases, the cutting force increases, and the cutting force decreases by decreasing the cutting Speed. Also, cutting force increases by 0 & 2 wt% of NP, and 1 wt% of NP decreases cutting force. It is happening due to the higher heat transfer rate of Al_2O_3 NP, which impacts the interface zone of the tool-workpiece and high heat rate generation at a quicker rate. Zno NP shows high stability in nanofluid, which makes it more likely to form a lubricant film for a longer time between the cutting tool and workpiece, thereby reducing the turning force.

The 3D response surface plot of wt% of NP and cutting Speed at a feed rate of 0.18 mm/rev is shown in Fig. 6. From it, the minimum cutting force is at cutting Speed 69.63 m/min and 1 wt% of NP. It can also be seen that the maximum amount of cutting force happens at 31.71 m/min and 0 wt% of NP.

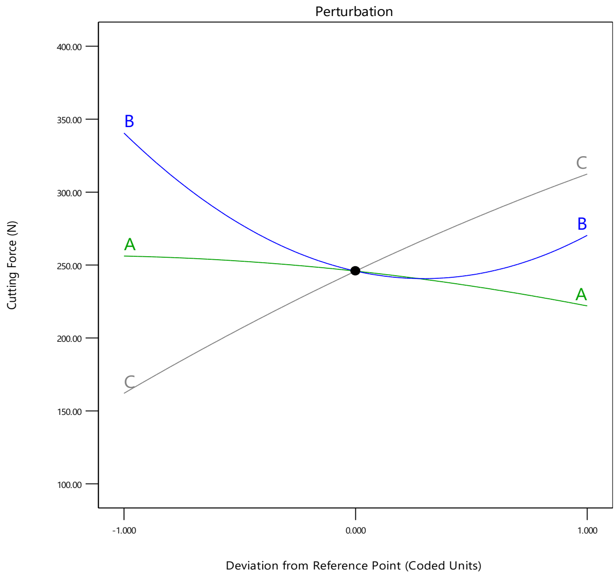

Fig. 5. Perturbation plot for cutting force.

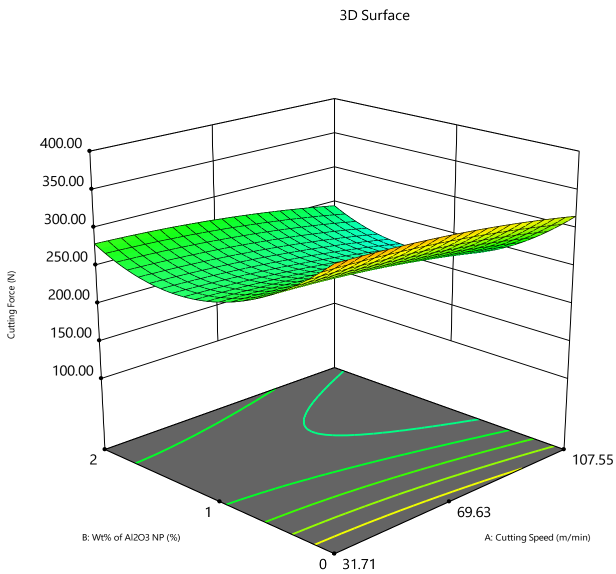

Fig. 6. 3D response surface plot cutting force vs cutting speed and %wt of NP.

3.1.2 Cutting temperature

For the cutting temperature response, the software predicts a quadratic model, and it is meaningful, as the p-value is less than 0.05. From Table 10, the ANOVA for cutting temperature indicates that cutting Speed, wt% of NP, and the square of wt% of NP are significant (p-value < 0.0001), and the interaction between the factors is not significant. This model is suitable for the output response cutting temperature derived from the data in Table 9. The Eq.2 shows final model for cutting temperature output response.

Table 10. ANOVA for cutting temperature.

Source	Sum of Squares	Mean Square	F-value	p-value	
Model	3282.38	364.71	54.21	< 0.0001	significant
A-Cutting Speed	468.33	468.33	69.62	< 0.0001	
B-Wt% of NP	1390.23	1390.23	206.66	< 0.0001	
C-Feed	190.22	190.22	28.28	0.0011	
AB	100.90	100.90	15.00	0.0061	
AC	0.8100	0.8100	0.1204	0.7388	
BC	3.71	3.71	0.5508	0.4821	
A^2	18.82	18.82	2.80	0.1384	
B^2	1121.24	1121.24	166.67	< 0.0001	
C^2	4.68	4.68	0.6953	0.4319	
Residual	47.09	6.73			
Lack of Fit	29.47	9.82	2.23	0.2271	not significant
Pure Error	17.62	4.41			
Cor Total	3329.47				

$$\begin{aligned} Cutting\ Temperature \\ &= 57.47 + 7.65 \times Cutting\ Speed + 13.18 \times wt\%\ of\ NP + 4.88 \times Feed \\ &- 5.02 \times Cutting\ Speed \times wt\%\ of\ NP - 0.45 \times Cutting\ Speed \times Feed \\ &- 0.9625 \times wt\%\ of\ NP \times Feed - 2.11\ (Cutting\ Speed)^2 + 16.32 \times (wt\%\ of\ NP)^2 \\ &- 1.05\ (Feed)^2 \end{aligned} \tag{2}$$

The normal probability plot for cutting temperature is shown in Fig. 7 and indicates that residuals have a close distance from the straight line. The terminology mentioned in the model is significant [19]. The externally studentized residuals versus run plot in Fig. 8 indicates a range of -4.8193 to 4.8193. It means this fitted model is suitable for cutting temperature response.

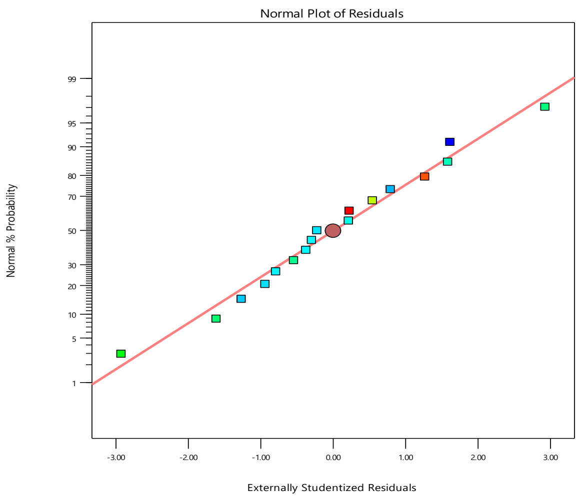

Fig. 7. Normal % probability plot for cutting temperature.

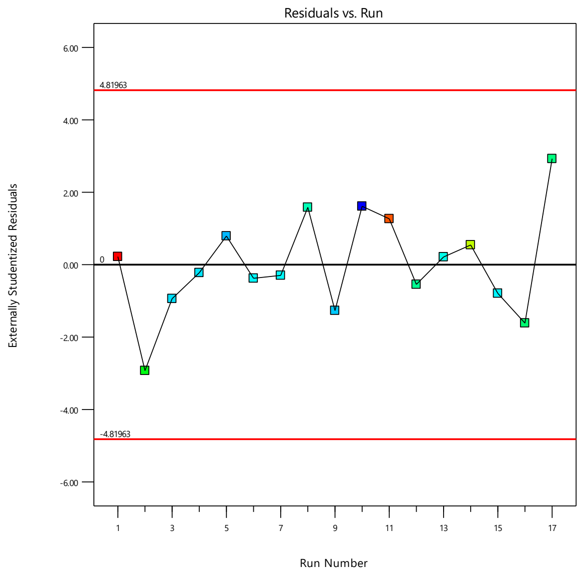

Fig. 8. Externally studentized residuals vs run of experiments.

Fig. 9 shows the effect of all input parameters: A: cutting Speed of 69.63 m/min, B: 1 wt% of NP, and C: feed of 0.18 mm/rev. As cutting Speed and feed rate increase, cutting temperature increases. Also, cutting temperature increases at 0 wt% of NP, and 1 wt% of NP decreases cutting temperature. Also, a slight increment in cutting temperature occurs when the value of wt% NP increased from 1 to 2. It is happening because Al_2O_3 NP has more heat transfer due to its higher thermal conductivity, which transfers heat very quickly.

The 3D response surface plot of wt% of NP and cutting Speed at a feed rate of 0.18 mm/rev is shown in Fig. 10. From it, the minimum cutting temperature is at cutting Speed 69.63 m/min and 1 wt% of NP. It can also be seen that the maximum amount of cutting temperature happens at 31.71 m/min and 0 wt% of NP.

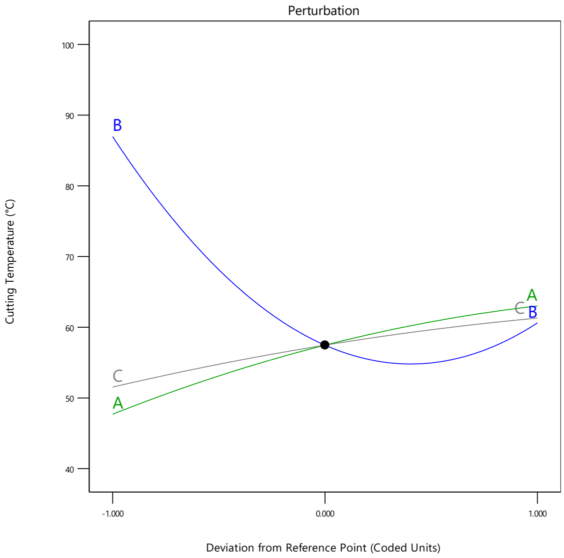

Fig. 9. Perturbation plot for cutting temperature.

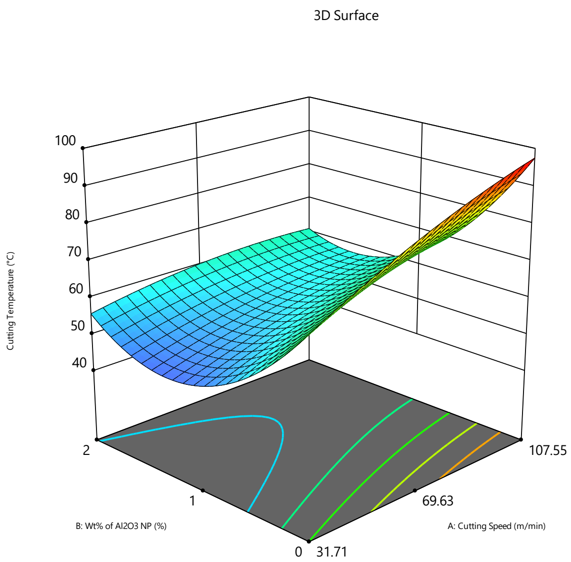

Fig. 10. 3D response surface plot cutting force vs cutting temperature and %wt of NP.

3.1.3 Surface Roughness

The last output response of the study is the surface roughness of the machined part, and the software predicts a second-order model. From Table 11, ANOVA for surface roughness is shown and indicates that feed and wt% of NP are more significant, and the interaction between the factors is not significant. This model is a suitable model for output response surface roughness drawn from data in Table 11. The Eq.3 shows final model for surface roughness output response.

Table 11. ANOVA for surface roughness.

Source	Sum of Squares	Mean Square	F-value	p-value	
Model	4.36	0.7261	35.27	< 0.0001	significant
A-Cutting Speed	0.2578	0.2578	12.52	0.0054	
B-Wt% of NP	0.7206	0.7206	35.01	0.0001	
C-Feed	3.00	3.00	145.51	< 0.0001	
AB	0.1132	0.1132	5.50	0.0410	
AC	0.2688	0.2688	13.06	0.0047	
BC	0.0008	0.0008	0.0381	0.8492	
Residual	0.2058	0.0206			
Lack of Fit	0.1735	0.0289	3.58	0.1187	not significant
Pure Error	0.0323	0.0081			
Cor Total	4.56				

$$\begin{aligned} Surace\ Roughness &= 4.13 + 0.1795 \times Cutting\ Speed + 0.3001 \times wt\%\ of\ NP + 0.6119 \times Feed \\ &+ 0.1683 \times Cutting\ Speed \times wt\%\ of\ NP - 0.2593 \times Cutting\ Speed \times Feed \\ &+ 0.0140 \times wt\%\ of\ NP \times Feed \end{aligned} \quad (3)$$

The normal probability plot for surface roughness is shown in Fig. 11 and indicates that residuals have a close distance from the straight line. The terminology mentioned in the model is significant [19]. The externally studentized residuals versus run plot in Fig. 12 indicates a point variation of -4.03715 to 4.03715 range. It means this fitted model is suitable for surface roughness response.

Fig. 13 shows the effect of all input parameters: A: cutting Speed of 69.63 m/min, B: 1 wt% of NP, and C: feed of 0.18 mm/rev. As cutting speed, feed rate, and wt% of NP increase, surface roughness increases. The 3D response surface plot of wt% of NP and cutting Speed at a feed rate of 0.18 mm/rev is shown in Fig. 14. From it, minimum surface roughness is at cutting Speed 31.71 m/min and 0 wt% of NP. It can also be seen that the maximum amount of surface roughness happens at 107.55 m/min and 2 wt% of NP.

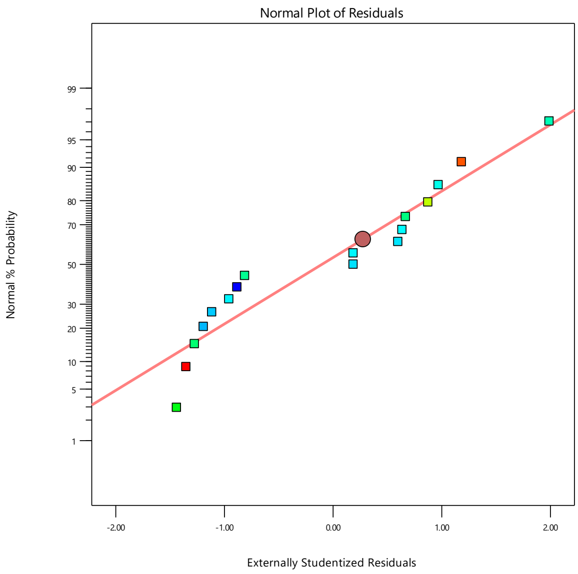

Fig. 11. Normal % probability plot for surface roughness.

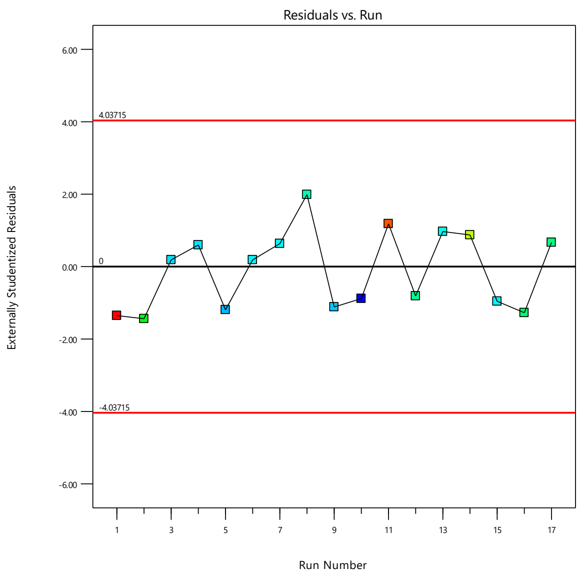

Fig. 12. Externally studentized residuals vs run of experiments.

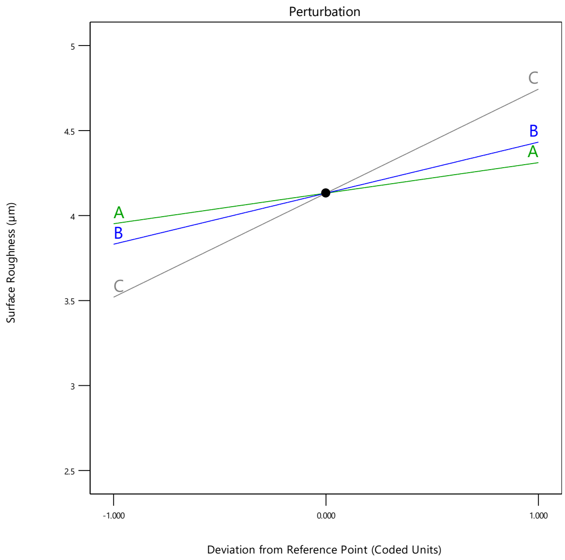

Fig. 13. Perturbation plot for surface roughness.

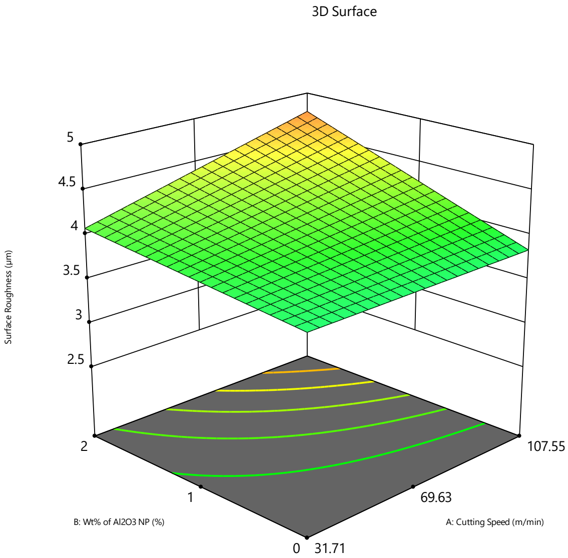

Fig. 14. 3D response surface plot surface roughness versus cutting speed and %wt of NP.

Experimentation results show that a 75:25 proportion mixing of Al_2O_3 and ZnO has obtained the best output responses for cutting force, cutting temperature, and surface roughness in comparison to other hybrid nano fluids and without the addition of nanoparticles. Addition of nanoparticles up to a moderate level, i.e., 1 wt%, to the base fluid increases the thermal conductivity of the nanofluid cutting fluid. This is a reason for a reduction in the value of output parameters in the turning operation. As reported by [18], the spherical shape of nanoparticles improved lubricating properties and acts as a joint between the tool and the chip. So, the combined effect of the cooling effect due to improved thermal conductivity and the lubricating phenomenon due to the joint bearing characteristic.

4. OPTIMIZATION AND VALIDATION

After statistical analysis of each input parameter on the output parameters was completed, the next step is to reach the optimum condition. Mane et al. [20] had suggested optimum conditions using Taguchi Analysis. In this research study, the optimal input and output parameter of the level was identified using the Box Behnken method for RSM. Once the optimum level of parameters was recognized, the final task is to validate the predicted outputs by performing a validation experiment. The aim of the validating experiment is to verify conclusions derived in the statistical analysis stage and the improvement of measured output performance using the optimum level.

The constraint criteria for input parameters, i.e., Cutting Speed, Wt% of NP, and Feed, have a goal of being in the range from lower to higher values, and output parameters, i.e., Cutting Force, Cutting Temperature, and Surface Roughness, have a goal of being minimum. Table 12 shows constraint criteria for parameters to get the optimum level.

Table 12. Criteria table for optimum condition.

Parameter	Goal	Lower Limit	Upper Limit	Lower Weight	Upper Weight
A:Cutting Speed	is in range	31.71	107.55	1	1
B:Wt% of NP	is in range	0	2	1	1
C:Feed	is in range	0.11	0.25	1	1
Cutting Force	minimize	148.757	392.24	1	1
Cutting Temperature	minimize	43.21	97.84	1	1
Surface Roughness	minimize	2.996	4.979	1	1

The optimal conditions at a high desirability value of 0.985 for Cutting Force, Cutting Temperature, and Surface Roughness are as follows: Cutting Speed: 31.71 m/min, Wt% of NP: 1, and Feed: 0.11. After the optimum condition is found for output parameters, the next step is to carry out confirmation experimentation, three runs with the use of each input parameter at the optimum level.

Table 13 indicates that experimentation runs extract the expected as well as actual answers and compare them with the predicted value. From comparisons of output results, it can be seen that predicted value and measured output parameters are in good agreement, which indicates that control parameter improvement is assured.

Table 13. Combination of optimum parameters for confirmation experimentation run.

Output Parameter	Optimum input level	Predicted value by RSM	Experiment value
Cutting Force	Cutting Speed: 31.71 m/min, Wt% of NP: 1 and Feed: 0.11 mm/rev	148.76	146.57
Cutting Temperature	Cutting Speed: 31.71 m/min, Wt% of NP: 1 and Feed: 0.11 mm/rev	41.0537	42.1
Surface Roughness	Cutting Speed: 31.71 m/min, Wt% of NP: 1 and Feed: 0.11 mm/rev	3.08594	3.082

5. CONCLUSION

In this research, experimentation turning of AISI 1040 steel was carried out using the Design of Experiments method, the RSM Box Behnken method for three input factors: cutting Speed, wt% of nanoparticle concentration, and feed, and three output responses: cutting temperature, cutting force, and surface roughness were identified. Process output parameters were analyzed for different cases, and case C (75:25, Al_2O_3:ZnO) was found to be the most suitable cutting condition. Based on the obtained results and discussion, this study draws the following conclusions:

1. The predicted Box Behnken regression model is in close agreement with the obtained results of experimentation runs. Also, the relationship between the output response variable and the independent control input variable is developed using RSM as a regression equation.
2. Cutting force and cutting temperature are mainly affected by cutting conditions. Both increase with an increase of cutting Speed, feed & wt% of nanoparticle because high thermal conductivity of Al_2O_3 NP, which impacts the interface zone of tool-workpiece and high heat rate generation at quicker rate and ZnO NP has high stability in nanofluid which make tendency to make lubricant film for more time between cutting tool & workpiece and as it leads a reduction in turning force.
3. As the cutting speed, feed, and wt% of the nanoparticle increase, surface roughness increases. MQL with hybrid nanofluid cutting fluid provides better surface finish than MQL as compared with conventional cutting conditions. This happened due to MQL with hybrid nanofluid taking away heat during turning and also providing a joint bearing effect, which resulted in improved anti-wear and anti-friction properties, and tends to improve surface quality.
4. Low cutting speed 31.71 m/min, low 0.11 mm/rev, and intermediate inclusion of nanoparticle, i.e., 1 wt%, has shown the best result. Optimization and validation for this optimal cutting condition had shown higher desirability, and predicted value and measured output had good agreement. So, a higher value of cutting Speed and feed increases the value of output parameters. Also, the addition of a higher weight percentage of nanoparticles in the nanofluid has not shown any significant effect on the output response.

Future studies may involve more process parameters like change in MQL pressure and flow rate, nozzle tip angle position, distance, and direction from the workpiece tool interface.

REFERENCES

[1] A. M. Khan *et al.*, "Multi-objective optimization for grinding of AISI D2 steel with Al_2O_3 wheel under MQL," *Materials*, vol. 11, no. 11, 2018, doi: 10.3390/ma11112269.

[2] L. B. Abhang and M. Hameedullah, "Experimental investigation of minimum quantity lubricants in alloy steel turning," *Int. J. Eng. Sci. Technol.*, vol. 2, no. 7, pp. 3045–3053, 2010.

[3] V. S. Sharma, G. Singh, and K. Sorby, "A review on minimum quantity lubrication for machining processes," *Mater. Manuf. Process.*, vol. 30, no. 8, pp. 935–953, Aug. 2015, doi: 10.1080/10426914.2014.994759.

[4] A. K. Sharma, A. K. Tiwari, and A. R. Dixit, "Effects of minimum quantity lubrication (MQL) in machining processes using conventional and nanofluid-based cutting fluids: A comprehensive review," *J. Clean. Prod.*, 2016, doi: 10.1016/j.jclepro.2016.03.146.

[5] R. K. Bumataria, N. K. Chavda, and H. Panchal, "Current research aspects in mono and hybrid nanofluid-based heat pipe technologies," *Heliyon*, vol. 5, no. 5, p. e01627, 2019, doi: 10.1016/j.heliyon.2019.e01627.

[6] R. K. Bumataria, N. K. Chavda, and A. H. Nalbandh, "Performance evaluation of the cylindrical shaped heat pipe utilizing water-based CuO and ZnO hybrid nanofluids," *Energy Sources A*, 2020, doi: 10.1080/15567036.2020.1832628.

[7] A. K. Sharma, R. K. Singh, A. R. Dixit, and A. K. Tiwari, "Novel uses of alumina–MoS_2 hybrid nanoparticle enriched cutting fluid in hard turning of AISI 304 steel," *J. Manuf. Process.*, vol. 30, pp. 467–482, Dec. 2017, doi: 10.1016/j.jmapro.2017.10.016.

[8] R. K. Singh, A. K. Sharma, A. R. Dixit, A. K. Tiwari, A. Pramanik, and A. Mandal, "Performance evaluation of alumina–graphene hybrid nano-cutting fluid in hard turning," *J. Clean. Prod.*, vol. 162, pp. 830–845, Sep. 2017, doi: 10.1016/j.jclepro.2017.06.104.

[9] A. K. Sharma, A. K. Tiwari, A. R. Dixit, R. K. Singh, and M. Singh, "Novel uses of alumina/graphene hybrid nanoparticle additives for improved tribological properties of lubricant in turning operation," *Tribol. Int.*, vol. 119, pp. 99–111, 2018, doi: 10.1016/j.triboint.2017.10.036.

[10] M. Jamil *et al.*, "Effects of hybrid Al_2O_3–CNT nanofluids and cryogenic cooling on machining of Ti–6Al–4V," *Int. J. Adv. Manuf. Technol.*, vol. 102, no. 9–12, pp. 3895–3909, 2019, doi: 10.1007/s00170-019-03485-9.

[11] Ç. V. Yıldırım, "Experimental comparison of the performance of nanofluids, cryogenic and hybrid cooling in turning of Inconel 625," *Tribol. Int.*, vol. 137, pp. 366–378, Sep. 2019, doi: 10.1016/j.triboint.2019.05.014.

[12] A. Thakur, A. Manna, and S. Samir, "Performance evaluation of different environmental conditions on output characteristics during turning of EN-24 steel," *Int. J. Precis. Eng. Manuf.*, vol. 20, no. 10, pp. 1839–1849, Oct. 2019, doi: 10.1007/s12541-019-00179-w.

[13] Thakur, A. Manna, and S. Samir, "Experimental investigation of nanofluids in minimum quantity lubrication during turning of EN-24 steel," *Proc. Inst. Mech. Eng. J*, vol. 234, no. 5, pp. 712–729, May 2019, doi: 10.1177/1350650119878286.

[14] S. Gugulothu and V. K. Pasam, "Experimental investigation to study the performance of CNT/MoS_2 hybrid nanofluid in turning of AISI 1040 steel," *Aust. J. Mech. Eng.*, 2020, doi: 10.1080/14484846.2020.1756067.

[15] P. B. Zaman, M. I. H. Tusar, and N. R. Dhar, "Selection of appropriate process inputs for turning Ti-6Al-4V alloy under hybrid Al_2O_3–MWCNT nanofluid-based MQL," *Adv. Mater. Process. Technol.*, 2020, doi: 10.1080/2374068X.2020.1812324.

[16] M. Sandeep Kumar, V. Vasu, and A. Venu Gopal, "Investigation of influence of hybrid nanofluid/MQL on surface roughness in turning Inconel-718," *Adv. Appl. Mech. Eng.*, 2020, doi: 10.1007/978-981-15-1201-8_120.

[17] M. Sandeep Kumar, V. Murali Krishna, and M. Kumar, "Investigation on influence of hybrid biodegradable nanofluids (CuO–ZnO) on surface roughness in turning AISI 1018 steel," *Mater. Today Proc.*, 2020, doi: 10.1016/j.matpr.2020.04.477.

[18] S. Haghnazari and V. Abedini, "Effects of hybrid Al_2O_3–CuO nanofluids on surface roughness and machining forces during turning AISI 4340," *SN Appl. Sci.*, vol. 3, no. 2, 2021, doi: 10.1007/s42452-020-04088-w.

[19] D. C. Montgomery, *Design and Analysis of Experiments*, 8th ed. Hoboken, NJ, USA: Wiley, 2013.

[20] P. A. Mane, P. A. Dhawale, S. Nipanikar, and A. N. Khadtare, "Predictive modeling of surface roughness, tool wear, and cutting temperature in high-speed turning under sustainable machining environments," *SAE Int. J. Mater. Manuf.*, vol. 19, no. 1, May 2025, doi: 10.4271/05-19-01-0007.

Abbreviations

Al_2O_3	Aluminium Oxide
ANOVA	Analysis of Variance
ZnO	Zinc Oxide
NP	Nanoparticle
NF	Nanofluid
HyNF	Hybrid nanofluid
DOE	Design of Experimentation
RSM	Response surface methodology
Wt%	Weight Fraction (%)